4-9-2004

Identification and Characterization of a Novel Human Myeloid Inhibitory C-type Lectin-like Receptor (MICL) That Is Predominantly Expressed on Granulocytes and Monocytes

Andrew S.J. Marshall
Sir William Dunn School of Pathology

Janet A. Willmen
Sir William Dunn School of Pathology

Hsi Hsien Lin
Sir William Dunn School of Pathology

David L. Williams
Quillen-Dishner College of Medicine, williamd@etsu.edu

Siamon Gordon
Sir William Dunn School of Pathology

See next page for additional authors

Citation Information

Marshall, Andrew S.J.; Willmen, Janet A.; Lin, Hsi Hsien; Williams, David L.; Gordon, Siamon; and Brown, Gordon D.. 2004. Identification and Characterization of a Novel Human Myeloid Inhibitory C-type Lectin-like Receptor (MICL) That Is Predominantly Expressed on Granulocytes and Monocytes. *Journal of Biological Chemistry*. Vol.279(15). 14792-14802. https://doi.org/10.1074/jbc.M313127200 PMID: 14739280 ISSN: 0021-9258

Identification and Characterization of a Novel Human Myeloid Inhibitory C-type Lectin-like Receptor (MICL) That Is Predominantly Expressed on Granulocytes and Monocytes

Creator(s)

Andrew S.J. Marshall, Janet A. Willmen, Hsi Hsien Lin, David L. Williams, Siamon Gordon, and Gordon D. Brown

THE JOURNAL OF BIOLOGICAL CHEMISTRY
Vol. 279, No. 15, Issue of April 9, pp. 14792–14802, 2004
Printed in U.S.A.

Identification and Characterization of a Novel Human Myeloid Inhibitory C-type Lectin-like Receptor (MICL) That Is Predominantly Expressed on Granulocytes and Monocytes*

Received for publication, December 2, 2003, and in revised form, January 9, 2004
Published, JBC Papers in Press, January 22, 2004, DOI 10.1074/jbc.M313127200

Andrew S. J. Marshall‡, Janet A. Willment‡, Hsi-Hsien Lin‡, David L. Williams§, Siamon Gordon‡, and Gordon D. Brown‡¶

From the ‡Sir William Dunn School of Pathology, University of Oxford, Oxford OX1 3RE, United Kingdom and the §Department of Surgery, James H. Quillen College of Medicine, Johnson City, Tennessee 37614

Inhibitory and activatory C-type lectin-like receptors play an important role in immunity through the regulation of leukocytes. Here, we report the identification and characterization of a novel myeloid inhibitory C-type lectin-like receptor (MICL) whose expression is primarily restricted to granulocytes and monocytes. This receptor, which contains a single C-type lectin-like domain and a cytoplasmic immunoreceptor tyrosine-based inhibitory motif, is related to LOX-1 (lectin-like receptor for oxidized low density lipoprotein-1) and the β-glucan receptor (Dectin-1) and is variably spliced and highly *N*-glycosylated. We demonstrate that it preferentially associates with the signaling phosphatases SHP-1 and SHP-2, but not with SHIP. Novel chimeric analyses with a construct combining MICL and the β-glucan receptor show that MICL can inhibit cellular activation through its cytoplasmic immunoreceptor tyrosine-based inhibitory motif. These data suggest that MICL is a negative regulator of granulocyte and monocyte function.

The functional balance of the immune system is regulated, in part, by inhibitory and activatory receptors found on all leukocytes as well as on many non-immune cells (1). Within these activatory and inhibitory receptor families, cytoplasmic consensus motifs have been identified and shown to associate with particular signaling mechanisms. These motifs include the immunoreceptor tyrosine-based activation motifs (ITAMs),[1] which become phosphorylated upon stimulation, sending their activatory signals through a variety of intracellular enzyme cascades and resulting in a wide range of cellular outcomes, and the immunoreceptor tyrosine-based inhibitory motifs (ITIMs), which suppress such activatory signals by recruiting phosphatase enzymes that dephosphorylate ITAMs as well as other components of the activatory pathways.

The array of inhibitory and activatory receptors expressed by natural killer cells has recently been the focus of much investigation (2). In humans, these receptors can be divided into two families: the Ig superfamily, including the killer cell Ig-like receptors (3) that bind classical major histocompatibility complex class I or HLA G (non-classical), and the C-type lectin-like family (4), including the NKG2 receptors, which bind the non-classical HLA E or other distantly related molecules that are up-regulated on stressed, transformed, or infected cells (5, 6).

The C-type lectin and lectin-like proteins are classified into 14 groups based on the arrangement of their C-type lectin-like domains (CTLDs).[2] In particular, group V receptors include the lectin-like NKG2 family mentioned above, but also a distinct subgroup of these receptors that are expressed predominantly on myeloid and endothelial cells (7). The members of this subgroup appear to bind diverse ligands, as exemplified by LOX-1 (lectin-like receptor for oxidized low density lipoprotein-1) (8) and the β-glucan receptor (BGR), which is an activatory phagocytic receptor for β-glucans (9).[3] Although they share structural homology with classical carbohydrate-binding C-type (Ca^{2+}-dependent) lectins (10), the group V molecules are termed C-type lectin-like because they lack the residues involved in Ca^{2+} coordination (11).

Here, we describe the identification and characterization of a myeloid inhibitory C-type lectin-like receptor (MICL), a novel group V C-type lectin-like receptor that contains an ITIM in its cytoplasmic tail and is most homologous to the LOX-1/BGR subgroup. We demonstrate that it is expressed at the cell surface and is highly *N*-glycosylated and that its expression is restricted to polymorphonuclear leukocytes (PMNs) and monocytes. We also show that it associates with the signaling phosphatases Src homology-2 domain-containing tyrosine phosphatase (SHP)-1 and SHP-2 and that it can inhibit cellular activation.

EXPERIMENTAL PROCEDURES

Cell Lines and Growth Conditions—NIH3T3 fibroblasts, RAW264.7 monocytes, and the PT67 and HEK293T-based Phoenix ecotropic retroviral packaging cell lines were maintained in Dulbecco's modified

* This work was supported by the Theodore Williams Scholarship, the Arthritis Research Council, the British Heart Foundation, the Medical Research Council, and the Wellcome Trust. The costs of publication of this article were defrayed in part by the payment of page charges. This article must therefore be hereby marked "*advertisement*" in accordance with 18 U.S.C. Section 1734 solely to indicate this fact.

The nucleotide sequence(s) reported in this paper has been submitted to the GenBank™/EBI Data Bank with accession number(s) AY498550, AY498551, and AY498552.

¶ To whom correspondence should be addressed: Sir William Dunn School of Pathology, University of Oxford, South Parks Rd., Oxford OX1 3RE, UK. Tel.: 44-1865-275-531; Fax: 44-1865-275-515; E-mail: gordon.brown@path.ox.ac.uk.

[1] The abbreviations used are: ITAM, immunoreceptor tyrosine-based activation motif; ITIM, immunoreceptor tyrosine-based inhibitory motif; CTLD, C-type lectin-like domain; LOX-1, lectin-like receptor for oxidized low density lipoprotein-1; BGR, β-glucan receptor; MICL, myeloid inhibitory C-type lectin-like receptor; PMN, polymorphonuclear leukocyte; SHP, Src homology-2 domain-containing tyrosine phosphatase; CHO, Chinese hamster ovary; HA, hemagglutinin; RT, reverse transcription; TNF-α, tumor necrosis factor-α; FITC, fluorescein isothiocyanate; PBS, phosphate-buffered saline; SHIP, Src homology-2 domain-containing inositol phosphatase; contig, group of overlapping clones.

[2] Available at ctld.glycob.ox.ac.uk/.

[3] J. Herre, A. S. J. Marshall, E. Caron, A. D. Edwards, D. L. Williams, E. Schweighoffer, V. L. Tybulewicz, C. Reis e Sousa, S. Gordon, and G. D. Brown, manuscript in preparation.

Eagle's medium (Invitrogen) supplemented with 10% heat-inactivated fetal calf serum, 100 units/ml penicillin, 0.1 mg/ml streptomycin, and 2 mM L-glutamine. CHO-K1 cells were grown in Ham's F-12 nutrient mixture, and CHO-Lec1 cells were grown in α-minimal essential medium with ribonucleosides and deoxyribonucleosides, both with the supplements described above. All cell lines were obtained from the cell bank of the Sir William Dunn School of Pathology, for except CHO-Lec1 (American Type Culture Collection CRL-1735) (12, 13), Phoenix ecotropic (a gift from Dr. Gary Nolan, Stanford University), and PT67 (Clontech).

In Silico Analysis—Sequence analyses were performed using several on-line tools.[4] Sequences were aligned with ClustalX (14); dendrogram analysis and percentage identities were calculated by DNAMAN Version 4.0 (Lynnon BioSoft).

Cloning and Generation of Stable Cell Lines—All routine nucleic acid manipulation techniques were performed essentially as described by Sambrook *et al.* (15). The complete MICL open reading frame was originally cloned into the pBluescript SK II$^+$ vector (Stratagene) from human peripheral blood mononucleocyte cDNA using the Advantage HF2-PCR kit (Clontech) with primers 5′-AAAGGATCCTCTTTACATATTCATCAATG-3′ and 5′-AAACTCGAGACACTCCTTAAATGTATTTG-3′. Hemagglutinin (HA) and V5 epitope tags (used as described below) were generated using adaptor duplex oligonucleotides as described previously (16).[5] All tags were inserted at the 3′-end of each sequence, corresponding to the C-terminal extracellular domain of each receptor. The MICL/BGR chimera was generated using overlap extension PCR (17) with primers 5′-CTACAACTGATGAGTAACTTCCTATCAAGAAATAAAG-3′ and 5′-TTTATTTCTTGATAGGAAGTTACTCATCAGTTGTAG-3′ such that the MICL 5′-sequence ran into the murine BGR sequence after 95 amino acids, translating as ^{MICL88}NISLQLMS$^{MICL95/BGR83}$NFLSRNKEN^{BGR91}. PCR was used to generate cytoplasmic mutant constructs from the V5-tagged full-length MICL/BGR chimera, including the truncated mutant, in which the 5′-end of the gene encoding the cytoplasmic tail (amino acids 1–39) was replaced with a start codon (AUG) and a Kozak sequence, and the ITIM mutant, in which the ITIM (VTYADL, amino acids 5–10) was mutated to VTFADL to inactivate the signaling domain. A schematic of all constructs (without epitope tags) that were used in these experiments is presented in Fig. 1. The fidelity of all clones was confirmed by sequencing.

To obtain stable cell lines, constructs were subcloned into the pFBneo (Stratagene) or pMXs-IP (a gift from Professor Toshio Kitamura, University of Tokyo) (18) retroviral vector; packaged into virions using HEK293T-based Phoenix ecotropic or PT67 cells as described previously (19); and transduced into NIH3T3, CHO-K1, CHO-Lec1, or RAW264.7 cells. RAW264.7 and CHO-K1 cells were pretreated with 0.2 μg/ml tunicamycin to increase transduction efficiency. All cell lines were used as non-clonal populations to reduce any founder effects and were generated and tested at least twice to confirm their phenotype. Stable cell lines were selected and maintained in 0.6 mg/ml Geneticin or 3 μg/ml puromycin.

RNA Blot Analysis and Reverse Transcription (RT)-PCR—Northern blotting was performed using a full-length MICL cDNA probe as described previously (19, 20). RNA isolation and RT-PCR were also performed as described previously (19), except that random hexamer primers were used for first-strand cDNA synthesis. Leukocytes were isolated from buffy coats (Bristol Blood Donor Services) and separated into adherent and non-adherent mononuclear cells using Ficoll-Paque™ Plus (Amersham Biosciences) and from fresh peripheral blood and separated into PMNs and total mononuclear leukocytes using Polymorphprep™ (Axis-Shield, Oslo, Sweden) according to the manufacturers' protocols.

Fluorescent Zymosan Binding and Internalization and Tumor Necrosis Factor-α (TNF-α) Assays—Fluorescence-based binding assays using fluorescein isothiocyanate (FITC)-labeled zymosan (Molecular Probes, Inc.) were performed as follows. NIH3T3 transfectants were plated at 2×10^5 cells/well in 24-well plates the day prior to each experiment. The cells were washed three times; 100 μg/ml laminarin (Sigma) was added when appropriate; and the cells were incubated for 20 min at 37 °C to allow inhibition of BGR (21). Following the addition of FITC-labeled zymosan (25 particles/cell), the cells were incubated at 37 °C in 5% CO_2 for 60 min. After washes to remove unbound particles, the cells were lysed in 3% Triton X-100, and the amount of FITC-labeled zymosan bound by the cells was quantified using a Titertek Fluoroskan II (Labsystems Group Ltd.) as described (21).

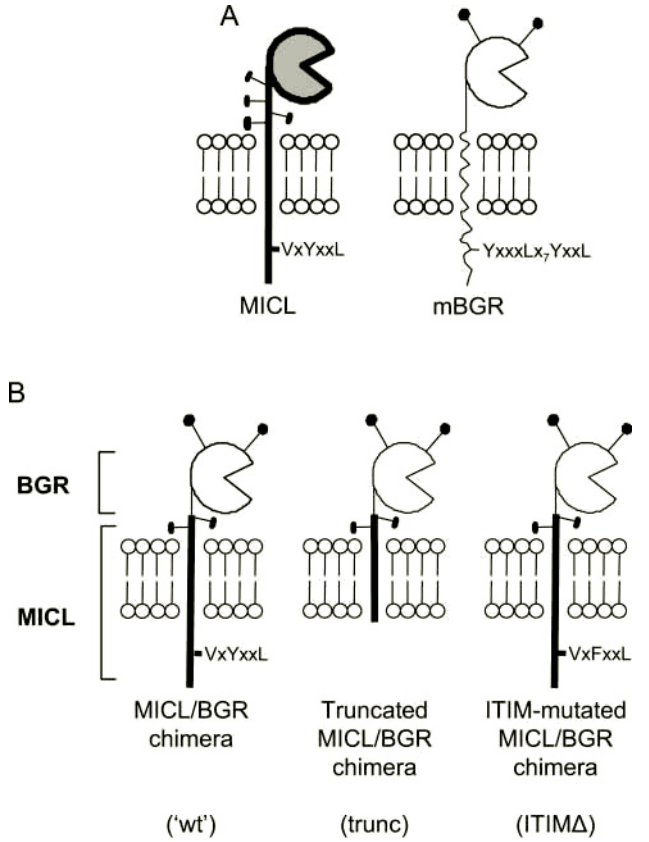

FIG. 1. **Schematic representation of the various constructs used in these experiments.** *A*, structures of both MICL and murine BGR (*mBGR*), showing a single CTLD, a stalk region, a single transmembrane domain, and a cytoplasmic tail containing an ITIM and an ITAM, respectively. *B*, the MICL/BGR chimera containing a wild-type MICL cytoplasmic tail and the murine BGR ectodomain (*wt*), the MICL/BGR chimera with a truncated cytoplasmic tail (*trunc*), and the MICL/BGR chimera with a mutated ITIM sequence (*ITIM*Δ). *N*-Glycosylation sites are indicated by the *lollipop structures*.

For the internalization assays, NIH3T3 transfectants were plated at 2×10^5 cells/well in 12-well plates the day prior to each experiment. At the start of the assay, the cells were washed three times with culture medium, and when necessary, cytochalasin D (1 μM; Sigma) was added to the cells 40 min prior to the start of the assay and then maintained throughout the experiment. Following the addition of FITC-labeled zymosan (5 particles/cell), the cells were incubated at 37 °C in 5% CO_2 for 30 min, washed to remove unbound particles, and then incubated for a further 90 min at 37 °C. External zymosan was stained with rabbit anti-zymosan antibody (Molecular Probes, Inc.) after blocking with phosphate-buffered saline (PBS) containing 1% bovine serum albumin and 5% heat-inactivated goat serum and then detected with allophycocyanin-conjugated goat anti-rabbit antibody (Molecular Probes, Inc.). The cells were lifted and fixed in 1% formaldehyde, and flow cytometry analysis (carried out according to conventional protocols) was performed by gating on the FITC-positive cell populations, which had bound zymosan. The percentage of phagocytosis was determined by comparing the allophycocyanin-negative (internalized particles) and allophycocyanin-positive (non-internalized particles) cell populations.

TNF-α production in RAW264.7 transfectants stimulated with zymosan was determined as described previously (16). After taking samples for anti-TNF-α enzyme-linked immunosorbent assay, the amount of FITC-labeled zymosan bound by the cells was quantified as described above. All graphical data are presented as the means ± S.D. from a representative experiment.

Immunoprecipitation—To identify MICL-associated phosphatases in RAW264.7 transfectants, cells were washed twice with PBS and resuspended in PBS containing 0.5% bovine serum albumin and 2 mM NaN_3. Aliquots containing 5×10^7 cells were incubated for 2 h at 4 °C with 5 μg of anti-HA antibody. Excess antibody was then removed by washing,

[4] Available at ca.expasy.org/, www.justbio.com/tools.php, and www.ncbi.nlm.nih.gov/BLAST/.

[5] Available at biochem.boehringer-mannheim.com/prod_inf/manuals/epitope/p20.pdf.

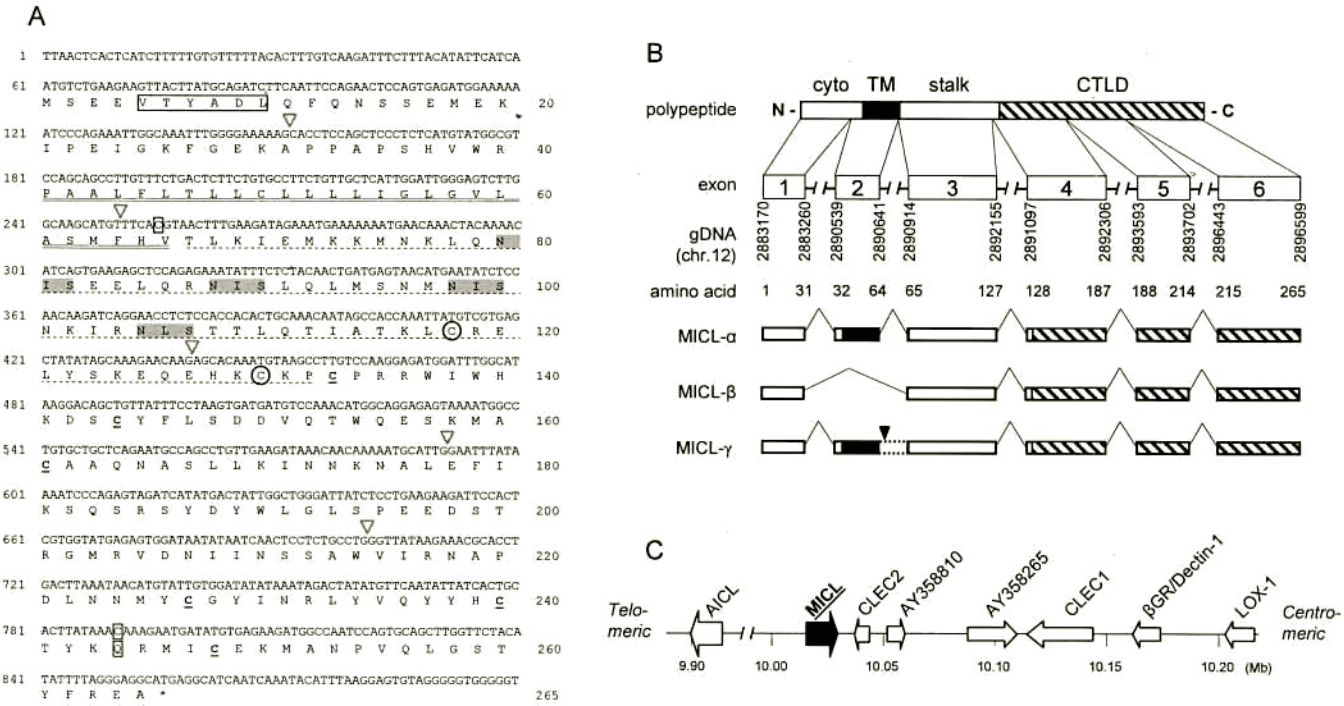

FIG. 2. **Structures of the MICL genomic, mRNA, and polypeptide sequences.** *A*, mRNA and predicted amino acid sequences of MICL. The 5′- and 3′-untranslated regions were derived from GenBank™/EBI accession number NM_138337 and overlapping expressed sequence tags. The ITIM is *boxed*; the predicted transmembrane domain is *double-underlined*; and the stalk region is *dashed-underlined*. High probability *N*-glycosylation sites in the stalk are *shaded*. *Circled* cysteines in the stalk region may allow homo-/heterodimerization through disulfide bridge formation (24); the cysteines that form the conserved CTLD are *underlined* and in *boldface*. Above the nucleotide sequence, exon boundaries are demarcated by *inverted triangles*, and single nucleotide polymorphisms are *boxed*; as a result of the second single nucleotide polymorphism, the *boxed glutamine* (*Q*) may be replaced with lysine. *B*, genomic structure of MICL aligned with the encoded polypeptide and three detected isoforms (see Fig. 4*B*). The genomic DNA (*gDNA*) positions of the exons on GenBank™/EBI contig NT_009714 from chromosome 12 (*chr. 12*) are indicated (untranslated regions are not shown). A premature stop codon created by alternative splicing in MICL-γ is indicated by an *inverted black triangle*. *cyto*, cytoplasmic tail; *TM*, transmembrane region. *C*, schematic view of part of human chromosome 12p13.31 including MICL (*black arrow*) and several closely related genes. A scale along the chromosome is shown in megabase pairs (*Mb*) from the start of the short arm. The mRNA and predicted polypeptide sequences of MICL-α, -β, and -γ have been submitted to the GenBank™/EBI Data Bank under accession numbers AY498550, AY498551, and AY498552, respectively. *βGR*, β-glucan receptor.

and the cells were resuspended in 2.25 ml of PBS and prewarmed to 37 °C for 3 min before stimulation with 250 μl of pervanadate (or PBS-only control), followed by incubation at 37 °C for 10 min. Pervanadate (22) was prepared from 1 mM activated Na_3VO_4 [6] and 10 mM H_2O_2 (final concentrations). Cells were lysed in Nonidet P-40 buffer (1% Nonidet P-40, 150 mM NaCl, 10 mM EDTA, 10 mM NaN_3, 10 mM Tris-HCl (pH 8), 2 mM Na_3VO_4, 10 mM NaF, and complete EDTA-free protease inhibitors (Roche Applied Science)) and incubated on ice for 45 min. Nuclei were pelleted at 12,000 × *g* for 20 min at 4 °C. Supernatants were added to 5 μl of anti-mouse Dynabeads® (precoated with 2% bovine serum albumin, Dynal Biotech) and incubated overnight at 4 °C. Beads were then washed four times with Nonidet P-40 buffer, and precipitated proteins were denatured by boiling for 5 min in reducing sample buffer. Aliquots were subjected to SDS-10% PAGE, and proteins were transferred to Hybond-C Extra membranes (Amersham Biosciences) for 90 min at 100 V. Proteins were probed with primary antibody in PBS containing 2% skimmed milk powder for 2 h at room temperature, followed by peroxidase-conjugated secondary antibody for 60 min at room temperature and detection using ECL substrate (Amersham Biosciences). The primary antibodies used were mouse anti-HA (HA.11, Covance), rabbit anti-SHP-1 (Upstate Biotechnology, Inc.), mouse anti-SHP-2 (clone 79, BD Biosciences) and rabbit anti-Src homology-2 domain-containing inositol phosphatase (SHIP) (a gift from Dr. Gerry Krystal).

RESULTS

MICL Is a C-type Lectin-like Transmembrane Receptor with a Cytoplasmic ITIM—We identified a novel human immunoreceptor that we named MICL (Fig. 2*A*) through data base searches for molecules homologous to BGR. The MICL gene consists of six exons and is located on the (+)-strand of chromosome 12 (locus 12p13.31) within the natural killer gene complex (23), spanning ~14 kb on GenBank™/EBI genomic contig NT_009714 (Fig. 2*B*). It is positioned at the telomeric end of a cluster of homologous genes that include *LOX-1*, BGR, *CLEC-1*, and *CLEC-2* (Fig. 2*C*) (7). The predicted open reading frame encodes a 265-amino acid type II transmembrane polypeptide with an expected mass of ~31 kDa and comprises one CTLD, a stalk/neck region, a single transmembrane domain, and a cytoplasmic tail containing an archetypal ITIM (Figs. 1*A* and 2*A*). The CTLD contains the six canonical cysteines, present in almost all C-type lectins; and in the stalk, there are two extra cysteines that may allow homo- or heterodimerization (24). The ectodomain also contains several putative *N*-glycosylation sites and one predicted *O*-glycosylation site.[7] Two single nucleotide polymorphisms in the coding region have been identified (at 255 and 790 bp in Fig. 2*A*), although only the latter one results in an amino acid substitution (Q244K). The Lys^{244} allele was previously deposited in the GenBank™/EBI Data Bank under accession number NM_138337, but its functional significance is not yet known.

MICL Shares Homology with LOX-1, BGR, CLEC-1, and CLEC-2 as Well as Other Inhibitory Receptors—MICL is most homologous to other human C-type lectin-like molecules on chromosome 12 that are found in the same cluster (Fig. 2*C*), including two novel transcripts with GenBank™/EBI acces-

[6] Available at www.upstate.com/misc/protocols.q.prot.e.activation/Activation+of+Sodium+Orthovanadate.

[7] Available at www.cbs.dtu.dk/services/NetNGlyc/ and www.cbs.dtu.dk/services/NetOGlyc/.

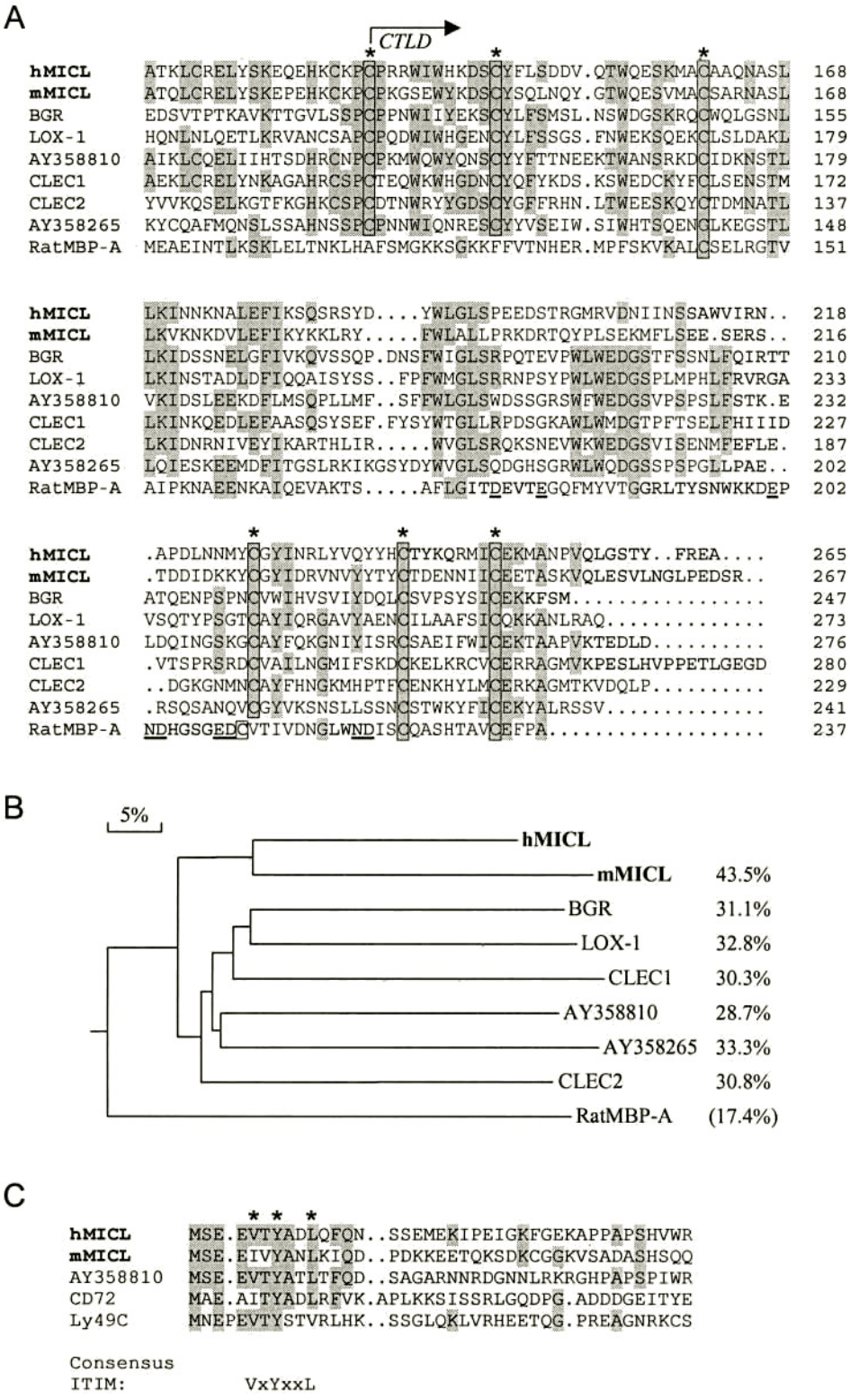

FIG. 3. **MICL is most homologous to the BGR/LOX-1/CLEC subgroup of C-type lectin-like molecules and to other ITIM-containing receptors.** *A*, alignment of the amino acid sequence of the human MICL (*hMICL*) CTLD with those of the murine ortholog (*mMICL*) and the most homologous human sequences. Rat MBP-A (mannose-binding protein-A) is included as a classical C-type lectin control, and its conserved calcium-binding residues (absent in the other C-type lectin-like sequences) are *underlined*. The sequences were obtained from the following accession numbers (from human MICL to rat MBP-A) and are numbered accordingly: GenBank™/EBI AY498550, NCBI XP_149798.2, NCBI CAC43847, NCBI BAA24580.1, GenBank™/EBI AY358810, NCBI NP_057595.2, NCBI NP_057593.1, GenBank™/EBI AAQ88632.1, and GenBank™/EBI AAA98781.1. Residues identical in >40% of the proteins are *shaded*; the canonic cysteines that make up the CTLD are *boxed* and indicated by *asterisks*. *B*, phylogenetic tree of the CTLDs of human and murine MICL and related human sequences. Values on the right indicate the percentage identity of each CTLD to the human MICL CTLD, and the distance scale indicates the percentage difference between the sequences. *C*, alignment of the cytoplasmic tail of human MICL with that of the murine ortholog and the first 20 residues of homologous ITIM-containing cytoplasmic tails. These were derived from the following accession numbers (from human MICL to Ly49C): GenBank™/EBI AY498550, AY358810, XP_149798.2, and AAH30227.1 and NCBI I49363. The positions of the conserved residues of the ITIMs are indicated by *asterisks* (full consensus sequence (V/I/L/S)xYxx(L/V/I/S) (73)).

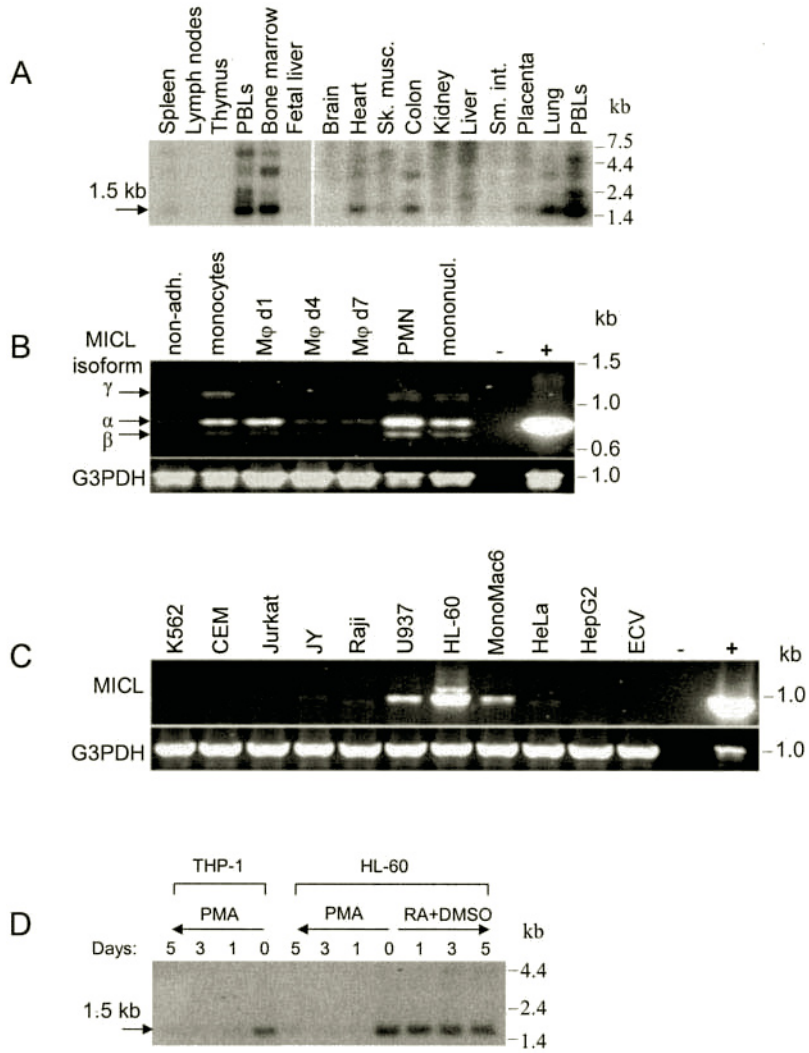

FIG. 4. **MICL mRNA is preferentially expressed in PMNs and monocytes.** *A*, Northern blots showing the expression of several MICL transcripts in immune and non-immune tissues. *PBLs*, peripheral blood leukocytes; *Sk. musc.*, skeletal muscle; *Sm. int.*, small intestine. *B*, RT-PCR analysis of leukocyte populations (non-adherent mononuclear leukocytes (*non-adh.*), monocytes, monocytes that were matured to macrophages over 7 days (*Mφ d1/d4/d7*), PMNs, and total mononuclear leukocytes (*mononucl.*)) showing expression of various isoforms (MICL-α/β/γ; see Fig. 2*B*) restricted to PMNs and monocytes. *C*, RT-PCR of various human cell lines demonstrating restricted expression of MICL transcripts in monocytic cell lines. RT-PCR controls for *B* and *C* are as follows: no template (−), cDNA from stable MICL-transfected RAW264.7 cells (+), and glyceraldehyde-3-phosphate dehydrogenase (*G3PDH*). *D*, Northern blot of total RNA from HL-60 and THP-1 cell lines showing down-regulation of MICL expression by phorbol 12-myristate 13-acetate (*PMA*) and maintenance of expression by all-*trans*-retinoic acid (*RA*) and dimethyl sulfoxide (*DMSO*). RNA loading controls for this blot were described previously (19).

sion numbers AY358265 and AY358810 (Fig. 3*A*). The predicted MICL CTLD sequence is most similar to those of AY358265, LOX-1, and BGR (Fig. 3*B*). Alignments of the CTLDs of MICL and related proteins show that they all contain the six conserved cysteines, but lack the Ca^{2+}-binding residues that are present in classical C-type lectins such as rat MBP-A (Fig. 3*A*). Furthermore, none of the known sugar-binding motifs present in classical C-type lectins, *e.g.* EPN/QPD (11), are found in MICL. Analysis of the MICL cytoplasmic tail revealed homology to other ITIM-containing group V C-type lectin-like molecules (Fig. 3*C*) such as AY358810, CD72, and murine Ly49C. The ITIM is also similar to those of certain better characterized type I transmembrane receptors, *viz.* signal-regulatory protein-α (SIRP-α), ILT5, KIR3DL1, and KIR2DL4 (data not shown).

Recently, the murine ortholog of MICL was identified (GenBank™/EBI accession number XM_149798). This gene is located within the equivalent gene cluster on the syntenic region of mouse chromosome 6. The encoded protein has 49% overall identity (~70% similarity) to human MICL and shares many of the features mentioned above, *e.g.* exon structure, *N*-glycosylation sites, and extra cysteines in the stalk. Similar MICL-related sequences are also present in other vertebrate genomes, including *Rattus norvegicus*, *Bos tauros*, and *Danio rerio* (data not shown).

MICL Has at Least Three Alternatively Spliced Transcripts, and Expression Is Restricted to PMNs and Monocytes—We examined the expression of human MICL by northern blotting and RT-PCR analysis. By northern blotting using a full-length cDNA probe, we were able to detect MICL transcripts in several tissues, especially those rich in leukocytes. One predominant transcript of 1.5 kb was observed in positive tissues, as were several transcripts of greater length. High levels of MICL transcripts were detected in peripheral blood leukocytes and bone marrow, with lower levels in spleen, fetal liver, heart, colon, placenta, and lung (Fig. 4*A*) as well as testis (data not shown). Blotting with an alternative MICL cDNA probe and increased hybridization stringency gave identical results, thus confirming the specificity of the hybridizing bands (data not shown).

We then determined the peripheral blood cell populations expressing MICL by RT-PCR and detected high levels of MICL transcripts in both PMNs and total mononuclear leukocytes (Fig. 4*B*). We separated the mononuclear leukocyte populations into non-adherent cells (predominantly lymphocytes) and adherent cells (predominantly monocytes), and the latter were also allowed to mature (from 1 to 7 days) into macrophages. MICL was detected in immature monocytes, but expression was gradually lost upon maturation toward macrophages; lymphocytes were MICL-negative. This experiment was repeated using blood from three separate donors, and comparable results were obtained, although the degree of MICL down-regulation concomitant with monocyte maturation was variable.

Several human cell lines from a range of sources were also analyzed for MICL expression. Consistent with previous data, only the monocytic/promyelocytic cells tested (U937, HL-60,

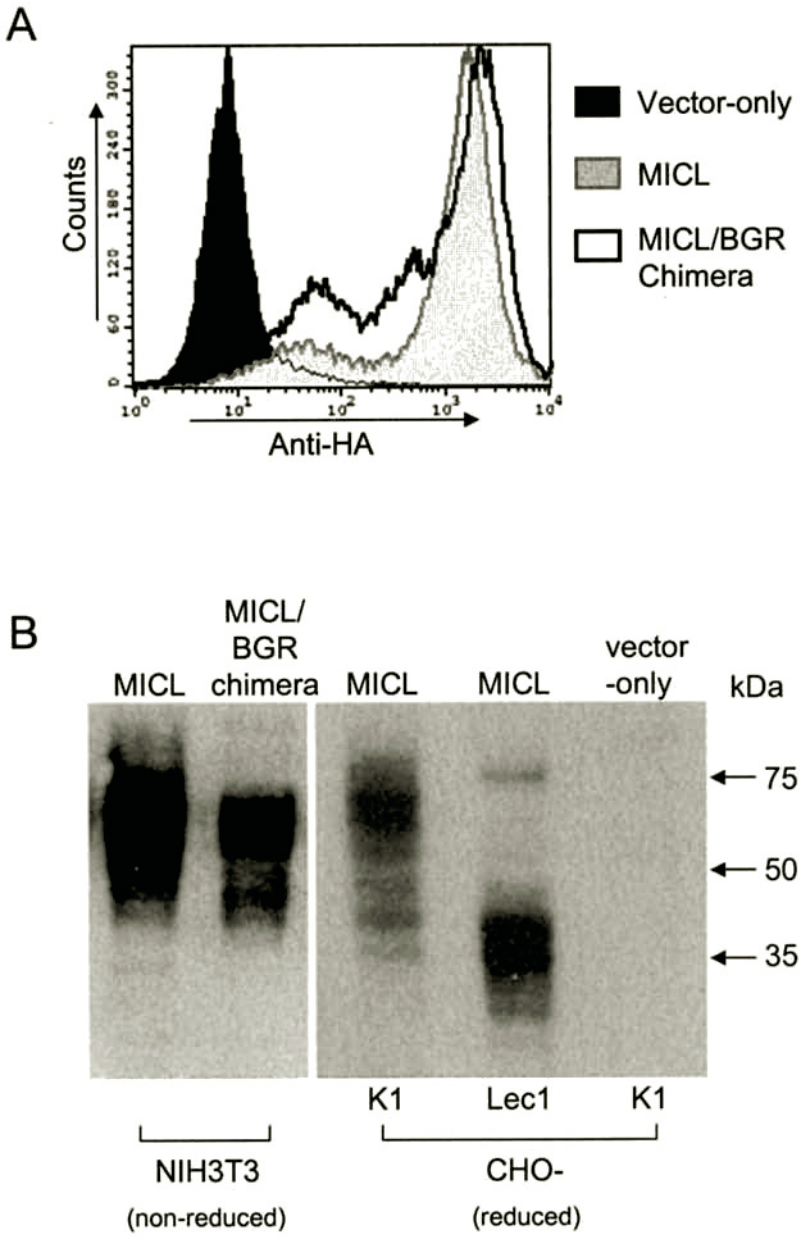

FIG. 5. **MICL-HA is expressed at the cell surface and is highly *N*-glycosylated when transfected into various cell lines.** *A*, flow cytometry of live (unpermeabilized) NIH3T3 cells stably expressing MICL or the MICL/BGR chimera with extracellular HA tags, demonstrating expression at the cell surface. A vector-only transfectant is shown as a control. *B*, anti-HA Western blots of nonreduced lysates from NIH3T3 transfectants, demonstrating a high level of glycosylation of both MICL and the MICL/BGR chimera because the bands on the reduced blots appear to be identical. Reduced lysates from wild-type (CHO-K1) cells and *N*-glycosylation-deficient (CHO-Lec1) transfectants show that the high molecular mass bands are due to *N*-glycosylation of MICL. Lysate from a vector-only transfectant is included as a blotting control.

and MonoMac6) were clearly MICL-positive (Fig. 4*C*). Moreover, maturation of the monocytic/promyelocytic cell lines THP-1 and HL-60 by phorbol 12-myristate 13-acetate, which induces a macrophage-like phenotype, down-regulated MICL expression as shown by northern blotting (Fig. 4*D*). In contrast, when HL-60 cells were treated with all-*trans*-retinoic acid and Me_2SO, which induce a PMN-like phenotype (25), MICL expression was maintained. This PMN/monocyte-restricted mRNA expression was further corroborated by SAGE,[8] which identified MICL transcripts in only myeloid cells, *viz.* granulocytes, monocytes, and immature dendritic cells (26, 27).[9] MICL was not detected in any SAGE library of lymphoid origin or in mature dendritic cells. All non-immune tissue libraries, except lung and liver, were also MICL-negative (28).[10] Thus, MICL appears to be expressed preferentially by granulocytes and monocytes.

RT-PCR analysis of peripheral blood leukocytes (Fig. 4*B*) identified three alternatively spliced isoforms of ~800, 700, and 1100 bp (MICL-α, -β, and -γ, respectively). These were cloned and sequenced, and their predicted structures are depicted in Fig. 2*B*. MICL-α is the isoform characterized in this work; MICL-β lacks exon 2 (encoding the transmembrane region); and in the MICL-γ transcript, the second intron is unspliced, resulting in the introduction of a stop codon after 18 codons. Transcripts similar to the MICL-γ isoform were also found in several human expressed sequence tags.

MICL Is Highly Glycosylated and Is Expressed at the Cell Surface—To investigate MICL protein expression and function, we generated HA epitope-tagged MICL transfectants in a variety of cell lines. Because several similar C-type lectin and lectin-like proteins are not expressed at the cell surface when transfected into certain cell lines (29, 30),[11] presumably due to the lack of accessory molecules, we examined the surface expression of MICL transfected into NIH3T3 fibroblasts (Fig. 5*A*).

[8] E. J. Evans, personal communication.
[9] Available at bloodsage.gi.k.u-tokyo.ac.jp/.
[10] Available at www.ncbi.nlm.nih.gov/SAGE.
[11] E. P. McGreal, G. D. Brown, S. Heinsbroek, S. Zamze, S. Y. Wong, S. Gordon, L. Martinez-Pomares, and P. R. Taylor, manuscript in preparation.

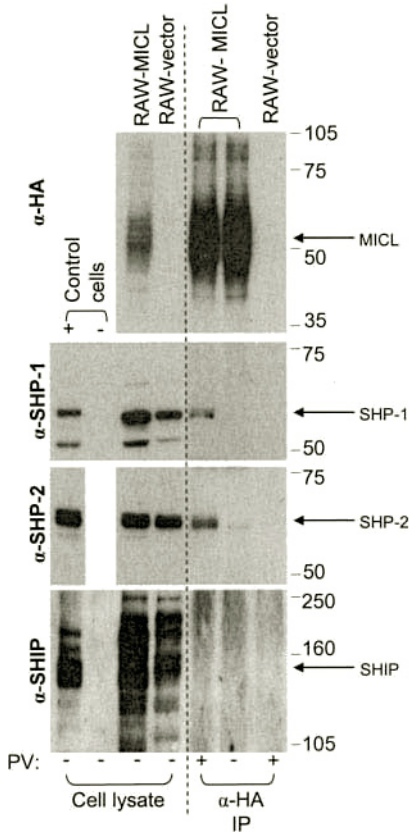

FIG. 6. **MICL associates with phosphatases SHP-1 and SHP-2 in RAW264.7 transfectants.** Shown are western blots of MICL-HA- or vector only-transfected RAW264.7 lysates and immunoprecipitates (*IP*) probed with antibodies as indicated. The anti-phosphatase (SHP-1/SHP-2/SHIP) Western blots indicate association of SHP-1 and SHP-2 (but not SHIP) with MICL upon pervanadate (*PV*) stimulation. Lysates, sufficient or deficient in the appropriate phosphatase enzyme, were also included as controls, except for a SHP-2-negative control. Untreated RAW264.7 transfectant cell lysates were analyzed to demonstrate the presence of each phosphatase. The anti-SHIP autoradiograph was overexposed to show that SHIP could not be detected in the immunoprecipitates. These data are representative of three independent experiments.

Analysis by flow cytometry of live transfected cells demonstrated high levels of MICL expression at the cell surface, indicating that accessory molecules were not required.

We also examined HA-tagged MICL expression by western blotting and observed bands between 40 and 75 kDa, which are much higher molecular masses than predicted from the polypeptide sequence alone (Fig. 5*B*). These bands were detected similarly under both reducing and nonreducing conditions in NIH3T3 and RAW264.7 lysates (data not all shown), suggesting they were due to glycosylation of MICL rather than dimerization. To confirm that MICL was glycosylated, we expressed MICL-HA in CHO-Lec1 cells, which are *N*-glycosylation-deficient (12, 13), as well as in wild-type CHO-K1 cells. CHO-K1 cells expressed glycosylated MICL in a similar fashion to NIH3T3 cells, but in CHO-Lec1 cells, the molecular mass of MICL was reduced to near its predicted unglycosylated mass (~31 kDa). Therefore, MICL is expressed at the cell surface and is highly *N*-glycosylated.

MICL Is Associated with SHP-1 and SHP-2, but Not with SHIP—ITIM-containing receptors are known to exact their inhibitory functions through the recruitment of phosphatase enzymes, including SHP-1, SHP-2, and SHIP (1). We therefore wanted to determine which, if any, of these phosphatases are recruited by the ITIM of MICL. To this end, we expressed HA-tagged MICL in RAW264.7 cells because this cell line is known to express all three phosphatases (31, 32) and isolated MICL-positive signaling complexes from these transfectants by anti-HA immunoprecipitation following treatment with and without pervanadate (Fig. 6), which stimulates recruitment of signaling molecules (22). Specific phosphatases that might associate with the MICL ITIM were identified by probing western blots of the immunoprecipitated complexes with selected anti-phosphatase antibodies. MICL-HA was observed to be expressed at the RAW 264.7 cell surface by flow cytometry (data not shown), and equal loading of MICL immunoprecipitates both with and without pervanadate was confirmed by anti-HA western blotting. Both SHP-1 and SHP-2 phosphatases were detected in pervanadate-stimulated MICL-positive immunoprecipitates, but not in unstimulated or MICL-negative controls. SHIP, which was present in multiple isoforms (33) in the untreated cell lysates, could not be detected in the MICL immunoprecipitates. These results indicate that MICL preferentially associates with SHP-1 and SHP-2.

The Cytoplasmic Tail of MICL Can Function in an Inhibitory Fashion—The ligands for MICL are not known; and therefore, to investigate the function of MICL, we generated a MICL/BGR chimera that could bind the BGR ligand zymosan. This chimera comprises the cytoplasmic tail, the transmembrane region, and part of the stalk of MICL fused with most of the murine BGR ectodomain (Fig. 1*B*). Cells stably expressing this chimeric construct have enabled us to dissociate the signaling functions of the MICL cytoplasmic tail (and ITIM) from those of its CTLD. We analyzed MICL/BGR chimeric transfectants by both flow cytometry, which demonstrated surface expression (Fig. 5*A*), and by western blotting, which revealed that the chimera has a molecular mass slightly lower than that of full-length MICL (Fig. 5*B*). Because this chimeric molecule contains the two most membrane-proximal *N*-glycosylation sites from the MICL stalk and given that the murine BGR component of this chimera does not contribute significantly to this *N*-glycosylation (34) (data not shown), we concluded that these two sites are responsible for the majority of the MICL glycosylation.

We first determined whether this chimeric construct (expressed in NIH3T3 cells) is functional for binding of β-glucan ligands. Cells transfected with MICL alone were unable to bind zymosan, whereas MICL/BGR chimeric transfectants were able to bind zymosan to a level comparable with that of cells expressing intact BGR (Figs. 1*A* and 7*A*). The BGR dependence of this binding was confirmed by specific blocking with the soluble β-glucan laminarin, demonstrating that the ectodomain of the MICL/BGR chimera is functionally intact.

We also utilized the MICL/BGR chimeric transfectants to examine the endocytic/phagocytic potential of MICL. Transfected NIH3T3 cells were allowed to bind and internalize FITC-labeled zymosan, and the amount of internalization was quantified as described under "Experimental Procedures." Cytochalasin D, which blocks actin polymerization, was included as a control in these experiments. Whereas >50% of the BGR-transfected cells were able to internalize the bound FITC-labeled zymosan, the MICL/BGR chimeric transfectants were unable to internalize their zymosan significantly above control levels (Fig. 7*B*). Furthermore, by fluorescence microscopy, FITC-labeled zymosan could be seen in rosettes around the MICL/BGR chimeric transfectants with little internalized, whereas almost all the BGR only-expressing cells had FITC-labeled zymosan within them (data not shown). Thus, the cytoplasmic tail of MICL does not mediate ligand uptake.

To demonstrate that the ITIM of MICL is a functional inhibitory domain, we also assessed the ability of the MICL/BGR chimera to block cellular activation. For these experiments, we coexpressed full-length BGR together with the MICL/BGR chi-

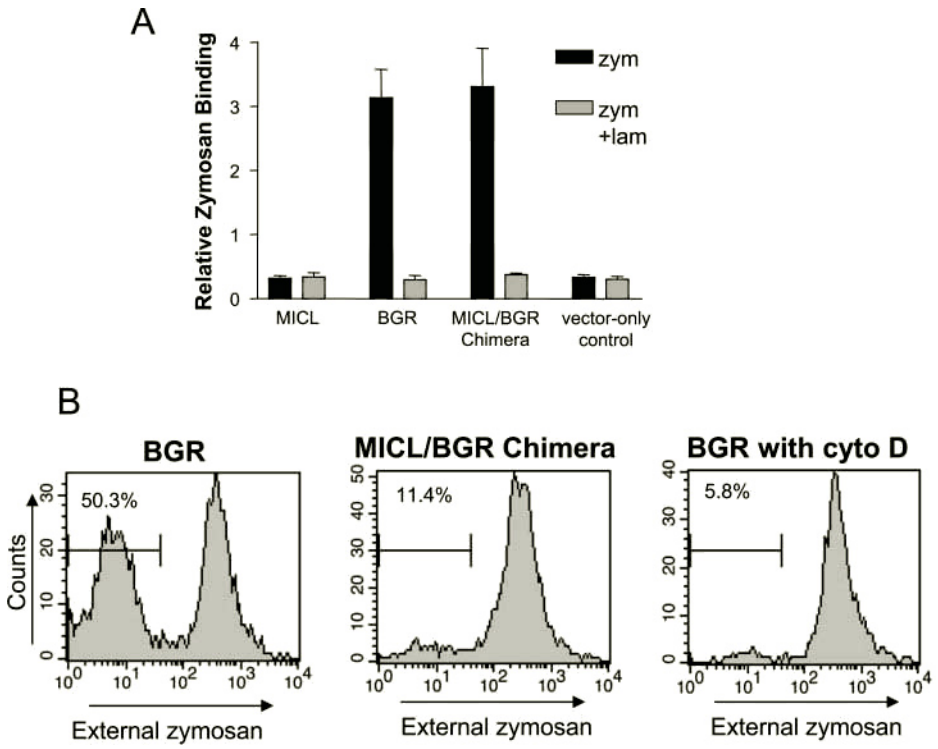

FIG. 7. **The MICL/BGR chimera is functional for zymosan binding, but cannot mediate internalization of the ligand.** *A*, in NIH3T3 transfectants, full-length MICL did not bind FITC-labeled zymosan (*zym*). In the MICL/BGR chimera, the BGR CTLD conferred on this construct the ability to bind zymosan to the same high level as full-length BGR. Inhibition of binding by laminarin (*lam*) indicates the β-glucan dependence of this interaction. *B*, shown are the results from anti-zymosan flow cytometry analysis of the internalization of zymosan by NIH3T3 transfectants expressing either intact BGR or the MICL/BGR chimera as described under "Experimental Procedures." Cytochalasin D (*cyto D*) was used to block internalization. Percentages indicate the proportion of cells that completely internalized the zymosan they bound. These data are representative of three independent experiments.

mera in RAW264.7 cells to examine the effect of the MICL ITIM on BGR ITAM-mediated cellular activation. Flow cytometric analysis confirmed that the doubly transfected cell line was expressing the desired constructs at the cell surface (Fig. 8*A*). The expression of BGR alone resulted in increased zymosan binding (Fig. 8*B*) compared with negative control transfectants and a concomitant increase in TNF-α production (Fig. 8*C*) as expected (16). However, although zymosan binding increased when the MICL/BGR chimera was coexpressed with BGR, the result of an increased number of zymosan-binding sites at the cell surface, TNF-α production was largely blocked, suggesting that the ITIM of the chimera was suppressing the activatory BGR signal. Coexpression of the MICL/BGR chimera with full-length BGR also significantly inhibited the level of zymosan internalization (data not shown).

To confirm that the inhibition by the chimera was dependent on the MICL ITIM and was not an artifact due to factors such as steric hindrance, we generated a MICL/BGR chimeric construct containing a truncated cytoplasmic domain (Fig. 1*B*, *trunc*) and a chimera in which the ITIM of MICL had been mutated (*ITIM*Δ). As described above, these constructs were coexpressed alongside full-length BGR, and cell-surface expression was confirmed by flow cytometry (Fig. 8*A*). For both of these transfectants, zymosan binding was increased as before (Fig. 8*B*), but TNF-α production was not inhibited (Fig. 8*C*). This demonstrates that MICL is a functional inhibitory receptor whose activity is dependent on its ITIM.

DISCUSSION

We present here the identification and initial characterization of a novel human inhibitory C-type lectin-like immunoreceptor. We have given it the acronym MICL for myeloid inhibitory C-type lectin-like receptor because we have shown that it bears a group V CTLD, has a predominantly PMN/monocyte-restricted expression pattern, and is functional as an inhibitory receptor. MICL shares many features with other C-type lectin-like receptors such as the NKG2 family (4), including a CTLD that conforms to the basic structure of classical C-type lectins, but in which the Ca^{2+}-binding residues are not conserved (Fig. 3*A*). MICL is, however, most homologous to a subgroup of C-type lectin-like molecules that are distinct from the NKG2 family and that are less well characterized, including BGR, LOX-1, and several novel receptors (7, 29). The ways in which the functions of the receptors in this subgroup relate to each other and to those of the NKG2 family, if at all, are not understood. The basic characterization of each member is a necessary first step toward elucidating the various *in vivo* roles of these molecules.

In the initial characterization of MICL expression, we have identified three isoforms (MICL-α, -β, and -γ) that result from alternative splicing (Figs. 2*B* and 4*B*). Several different transcripts of up to 6 kb were detected by northern blotting (Fig. 4*A*), suggesting that there are splice variants other than MICL-α/β/γ (*cf.* GenBank™/EBI cDNA clone BC027967.1). Many molecules homologous to MICL are also variably spliced (5, 19, 35–37), although the functional significance of most of their alternative isoforms has not yet been investigated. The MICL-β splice variant, which lacks the transmembrane region, is equivalent to isoforms of other C-type lectins that have been reported to be either secreted (38) or withheld in the cytosol (39). It has been suggested that alternative transcripts such as MICL-β and MICL-γ may encode dominant-negative inhibitors of full-length polypeptides (40). The relative levels of these alternative transcripts may be variably regulated in different cells under different conditions. For example, it appears that human BGR is expressed in monocytes/macrophages in only one of its two main isoforms, whereas both mRNA transcripts are expressed by PMNs (19). Similarly, CLECSF6, a group II C-type lectin expressed in several leukocyte populations including PMN and monocytes (41), has stalked and stalkless isoforms that appear to be oppositely regulated by anti- and pro-inflammatory stimuli (35).

The particular PMN/monocyte-restricted expression pattern of MICL (Fig. 4) is shared by few other, if any, ITIM-containing receptors; and therefore, MICL is likely to have a role distinct from those of other myeloid inhibitory molecules. Other human ITIM-containing receptors expressed on PMNs/monocytes as

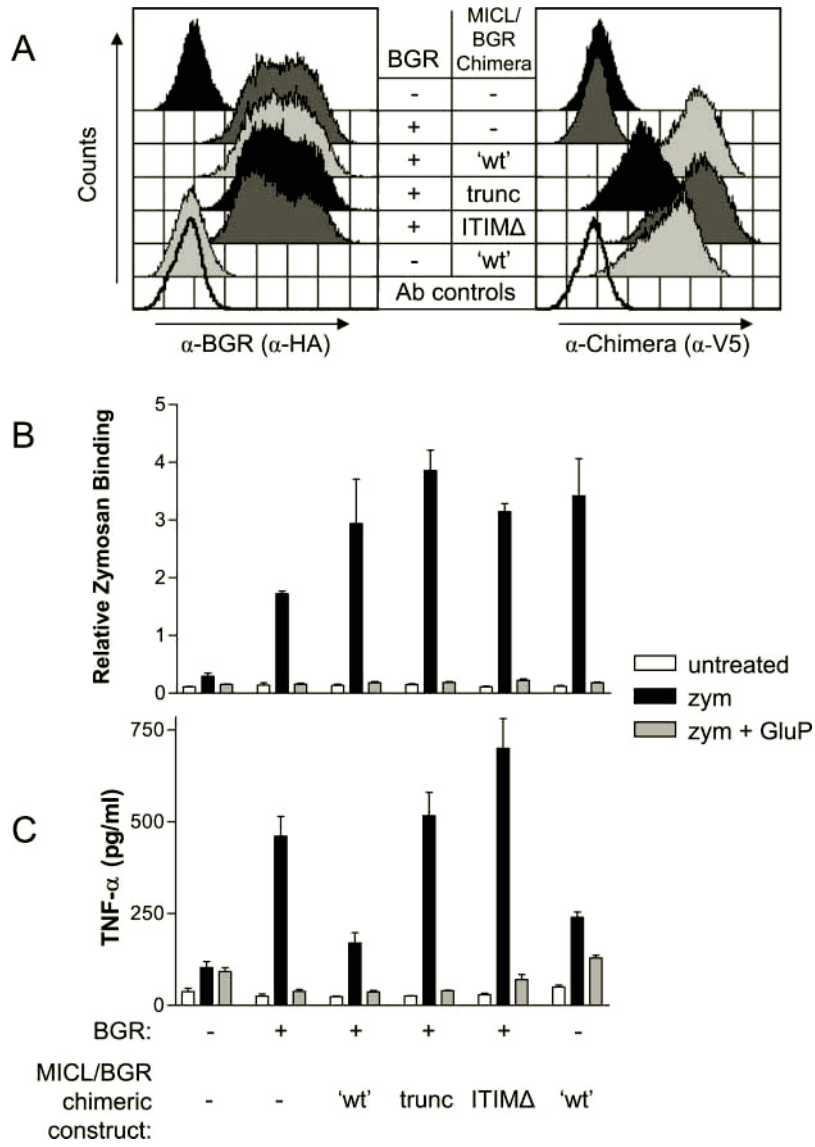

FIG. 8. **MICL can inhibit cellular activation through its ITIM.** *A*, live flow cytometric analysis to indicate the surface coexpression of BGR and various MICL/BGR chimeric constructs stably expressed in RAW264.7 cells. The BGR constructs were HA-tagged, and the chimeric constructs were V5-tagged. *wt*, the MICL/BGR chimera containing a wild-type MICL cytoplasmic tail and the murine BGR ectodomain; *trunc*, the MICL/BGR chimera with a truncated cytoplasmic tail; *ITIM*Δ, the MICL/BGR chimera with a mutated ITIM sequence; *Ab*, antibody. *B*, quantification of FITC-labeled zymosan bound by each double transfectant, showing that the levels for the BGR and chimeric cotransfectants are above those of the BGR and vector-only control (−). *C*, concentration of TNF-α released by the RAW264.7 double transfectants following incubation with zymosan (*zym*) as determined by anti-TNF-α enzyme-linked immunosorbent assay. Only the chimera with a wild-type MICL ITIM (*wt*) was able to inhibit BGR-induced TNF-α production. These data are representative of three independent experiments in at least two sets of separately generated stable cell lines (74). *GluP*, glucan phosphate.

well as on a broad range of other cell populations include Fcγ receptor type IIB (42), members of the Siglec (43) and ILT families (44), signal-regulatory protein-α (45), MAFA-L (37), CLECSF6 (41), LAIR-1 (46), PD-1 (47), TLT-1 (48), FDF03 (49), and LMIR1 (50). These inhibitory receptors have been implicated in apoptosis (51), allergy (52), autoimmune disease (53), and cancer (54, 55). The variety of inhibitory effects reported to be mediated by these receptors includes inhibition of cell maturation (56), calcium mobilization (57), secretion/exocytosis (58), phagocytosis (59), cytokine production (56), and cellular proliferation (57). It is also notable that a few of the above receptors have seemingly "activatory" roles (some are suggested to promote cell migration (45), cell fusion (60), or apoptosis (55)) presumably in correlation with the function of the pathways they are inhibiting. As an inhibitory receptor preferentially expressed on PMNs/monocytes (Fig. 4), we can speculate that MICL might play a role similar to those above, such as preventing inappropriate migration or activation. It is striking that MICL was down-regulated concomitant with monocyte maturation (Fig. 4, *B* and *D*), a pattern that is inverse to that observed for the related activatory receptor BGR (19, 61, 62). This may provide a mechanism for removing the inhibitory effect of MICL on unstimulated monocytes so that they can become activated. The possibility of a similar down-regulation upon PMN activation has not yet been examined.

Analysis of the predicted MICL polypeptide sequence revealed that the cytoplasmic tail contains a consensus ITIM (Fig. 3*C*). The ITIMs of receptors such as MICL orchestrate their inhibitory effects by associating with one or more phosphatases, including SHP-1, SHP-2, and SHIP (1). Other inhibitory C-type lectin or lectin-like receptors have been found to preferentially associate with SHP-1 and/or SHP-2 (63), but not usually with SHIP (MAFA-L is one exception (37)). Consistent with this bias, we observed that MICL bound only SHP-1 and SHP-2 (Fig. 6). It is almost certainly via these phosphatases that the MICL ITIM exerts its inhibitory potential, as described below.

Following expression analyses and the identification of the signaling phosphatases associating with MICL, we demonstrated the inhibitory function of MICL using a MICL/BGR chimeric construct in which most of the ectodomain of MICL was replaced with that of BGR. Similar approaches have been employed previously, for example, to demonstrate the functioning of inhibitory receptors that can suppress activatory Fc receptors or B-cell activation (64, 65). We have made use of an established activatory pathway in RAW264.7 cells in which BGR, following binding of zymosan, is able to induce cellular activation, including TNF-α production and phagocytosis (16). In other immunoreceptor systems, co-clustering of an inhibitory receptor with an activatory receptor results in suppression

of activatory signals (66). Because both BGR and our MICL/BGR chimera could bind zymosan (Fig. 7*A*), coexpression of the two constructs allowed us to assess the ability of the chimera, following zymosan-induced co-clustering with BGR, to suppress BGR-dependent TNF-α induction and phagocytosis. By this approach, we were successful in demonstrating MICL-mediated inhibitory function. We also tested two modified MICL/BGR chimeras, one with the cytoplasmic tail truncated and another with a mutated ITIM, to show that inhibition of BGR signaling by the MICL component of the chimera was not due to steric hindrance, for example, but required active inhibition mediated by the MICL ITIM. Although this *in vitro* model demonstrates that MICL can function as an inhibitory receptor, the true function of MICL *in vivo* can be established only following the identification of its ligand.

Several other group V C-type lectin-like molecules (the NKG2 receptors) appear to bind non-classical major histocompatibility complex class I or related ligands, but because the MICL CTLD has low sequence identity to members of this subfamily (data not shown), it is probable that it does not bind a similar ligand. For example, CLEC-2, which is homologous to MICL, could not be demonstrated to bind a range of soluble class I tetramers (29). From what little is known about the ligands of the LOX-1, BGR, and CLEC cluster of receptors, it appears that, unlike those of the NKG2 subgroup, they are structurally unrelated. LOX-1 is reported to bind aged apoptotic cells, activated platelets, bacteria, and oxidized low density lipoprotein (8, 67), whereas BGR binds β-glucans as well as an unidentified T-cell antigen (19, 34). It can also not be assumed that MICL will bind protein rather than carbohydrate (9, 68–70) or act as a scavenger receptor (8). It is even possible that MICL binds another C-type lectin, as was recently found for Nkrp1d and Clrb (71).

Consistent with our ideas above concerning the function of MICL, we could suggest that an endogenous ligand for MICL might be expressed in a context in which PMN/monocytes should not normally be activated, such as at sites of immune privilege or within the blood. We have unsuccessfully screened various cell lines and tissues for a ligand using the MICL ectodomain multimerized on fluorescent beads, as previously employed in other ligand searches (72). We are currently employing alternative approaches to identify a ligand. The fact that MICL is substantially *N*-glycosylated (Figs. 5*B* and 6) may well have implications for ligand binding, as previously demonstrated for LOX-1 (70) and Ly49 (69), especially because the level of MICL *N*-glycosylation is much higher than the *N*-glycosylation level of homologous receptors, *e.g.* LOX-1 (70) and BGR (34) (data not shown). Another determinant of the ligand-binding potential of MICL is the possibility of homo- or heterophilic dimerization. Many other group V receptors dimerize through cysteines in the stalk region,[2] and although MICL does contain the necessary residues (Fig. 2), we have not identified any multimerized forms of this receptor. In conclusion, our preliminary characterization of MICL, its expression, and the demonstration of its functional potential provide the basis for future investigations aimed at identifying the ligand(s) and physiological function of MICL.

Acknowledgments—We thank Drs. Philip Taylor, Jurgen Herre, Ed Evans, Martin Stacey, Gary Brooke, Marion Brown, Yunpeng Su, Gerry Krystal, Laura Sly, Toshio Kitamura, and Gary Nolan for reagents and advice.

REFERENCES

1. Long, E. O. (1999) *Annu. Rev. Immunol.* **17,** 875–904
2. McQueen, K. L., and Parham, P. (2002) *Curr. Opin. Immunol.* **14,** 615–621
3. Vilches, C., and Parham, P. (2002) *Annu. Rev. Immunol.* **20,** 217–251
4. Lopez-Botet, M., and Chambers, W. H. (1996) *Methods* (*Orlando*) **9,** 352–361
5. Diefenbach, A., Tomasello, E., Lucas, M., Jamieson, A. M., Hsia, J. K., Vivier, E., and Raulet, D. H. (2002) *Nat. Immunol.* **3,** 1142–1149
6. Diefenbach, A., Hsia, J. K., Hsiung, M. Y., and Raulet, D. H. (2003) *Eur. J. Immunol.* **33,** 381–391
7. Sobanov, Y., Bernreiter, A., Derdak, S., Mechtcheriakova, D., Schweighofer, B., Duchler, M., Kalthoff, F., and Hofer, E. (2001) *Eur. J. Immunol.* **31,** 3493–3503
8. Mehta, J. L., and Li, D. (2002) *J. Am. Coll. Cardiol.* **39,** 1429–1435
9. Brown, G. D., and Gordon, S. (2001) *Nature* **413,** 36–37
10. Drickamer, K. (1993) *Biochem. Soc. Trans.* **21,** 456–459
11. Weis, W. I., Taylor, M. E., and Drickamer, K. (1998) *Immunol. Rev.* **163,** 19–34
12. Stanley, P., Caillibot, V., and Siminovitch, L. (1975) *Cell* **6,** 121–128
13. Stanley, P., Narasimhan, S., Siminovitch, L., and Schachter, H. (1975) *Proc. Natl. Acad. Sci. U. S. A.* **72,** 3323–3327
14. Thompson, J. D., Gibson, T. J., Plewniak, F., Jeanmougin, F., and Higgins, D. G. (1997) *Nucleic Acids Res.* **25,** 4876–4882
15. Sambrook, J., Fritsch, E. F., and Maniatis, T. (1989) *Molecular Cloning: A Laboratory Manual*, 2nd Ed., Cold Spring Harbor Laboratory, Cold Spring Harbor, NY
16. Brown, G. D., Herre, J., Williams, D. L., Willment, J. A., Marshall, A. S., and Gordon, S. (2003) *J. Exp. Med.* **197,** 1119–1124
17. Ho, S. N., Hunt, H. D., Horton, R. M., Pullen, J. K., and Pease, L. R. (1989) *Gene* (*Amst.*) **77,** 51–59
18. Kitamura, T., Koshino, Y., Shibata, F., Oki, T., Nakajima, H., Nosaka, T., and Kumagai, H. (2003) *Exp. Hematol.* **31,** 1007–1014
19. Willment, J. A., Gordon, S., and Brown, G. D. (2001) *J. Biol. Chem.* **276,** 43818–43823
20. Stacey, M., Lin, H.-H., Hilyard, K. L., Gordon, S., and McKnight, A. J. (2001) *J. Biol. Chem.* **276,** 18863–18870
21. Brown, G. D., Taylor, P. R., Reid, D. M., Willment, J. A., Williams, D. L., Martinez-Pomares, L., Wong, S. Y., and Gordon, S. (2002) *J. Exp. Med.* **196,** 407–412
22. Swarup, G., Cohen, S., and Garbers, D. L. (1982) *Biochem. Biophys. Res. Commun.* **107,** 1104–1109
23. Yokoyama, W. M., and Plougastel, B. F. (2003) *Nat. Rev. Immunol.* **3,** 304–316
24. Lazetic, S., Chang, C., Houchins, J. P., Lanier, L. L., and Phillips, J. H. (1996) *J. Immunol.* **157,** 4741–4745
25. Collins, S. J., Bodner, A., Ting, R., and Gallo, R. C. (1980) *Int. J. Cancer* **25,** 213–218
26. Evans, E. J., Hene, L., Sparks, L. M., Dong, T., Retiere, C., Fennelly, J. A., Manso-Sancho, R., Powell, J., Braud, V. M., Rowland-Jones, S. L., McMichael, A. J., and Davis, S. J. (2003) *Immunity* **19,** 213–223
27. Hashimoto, S., Nagai, S., Sese, J., Suzuki, T., Obata, A., Sato, T., Toyoda, N., Dong, H. Y., Kurachi, M., Nagahata, T., Shizuno, K., Morishita, S., and Matsushima, K. (2003) *Blood* **101,** 3509–3513
28. Lash, A. E., Tolstoshev, C. M., Wagner, L., Schuler, G. D., Strausberg, R. L., Riggins, G. J., and Altschul, S. F. (2000) *Genome Res.* **10,** 1051–1060
29. Colonna, M., Samaridis, J., and Angman, L. (2000) *Eur. J. Immunol.* **30,** 697–704
30. Bellon, T., Heredia, A. B., Llano, M., Minguela, A., Rodriguez, A., Lopez-Botet, M., and Aparicio, P. (1999) *J. Immunol.* **162,** 3996–4002
31. Angata, T., Kerr, S. C., Greaves, D. R., Varki, N. M., Crocker, P. R., and Varki, A. (2002) *J. Biol. Chem.* **277,** 24466–24474
32. Lucas, D. M., and Rohrschneider, L. R. (1999) *Blood* **93,** 1922–1933
33. Damen, J. E., Liu, L., Ware, M. D., Ermolaeva, M., Majerus, P. W., and Krystal, G. (1998) *Blood* **92,** 1199–1205
34. Ariizumi, K., Shen, G. L., Shikano, S., Xu, S., Ritter, R., III, Kumamoto, T., Edelbaum, D., Morita, A., Bergstresser, P. R., and Takashima, A. (2000) *J. Biol. Chem.* **275,** 20157–20167
35. Richard, M., Veilleux, P., Rouleau, M., Paquin, R., and Beaulieu, A. D. (2002) *J. Leukocyte Biol.* **71,** 871–880
36. Huang, X., Yuan, Z., Chen, G., Zhang, M., Zhang, W., Yu, Y., and Cao, X. (2001) *Biochem. Biophys. Res. Commun.* **281,** 131–140
37. Abramson, J., Xu, R., and Pecht, I. (2002) *Mol. Immunol.* **38,** 1307–1313
38. Ishiwata, N., Takio, K., Katayama, M., Watanabe, K., Titani, K., Ikeda, Y., and Handa, M. (1994) *J. Biol. Chem.* **269,** 23708–23715
39. Fernandes, M. J., Iscove, N. N., Gingras, G., and Calabretta, B. (2000) *Genomics* **69,** 263–270
40. Furukawa, H., Yabe, T., Watanabe, K., Miyamoto, R., Akaza, T., Tadokoro, K., Tohma, S., Inoue, T., Yamamoto, K., and Juji, T. (1998) *Immunogenetics* **48,** 87–88
41. Bates, E. E., Fournier, N., Garcia, E., Valladeau, J., Durand, I., Pin, J. J., Zurawski, S. M., Patel, S., Abrams, J. S., Lebecque, S., Garrone, P., and Saeland, S. (1999) *J. Immunol.* **163,** 1973–1983
42. Brooks, D. G., Qiu, W. Q., Luster, A. D., and Ravetch, J. V. (1989) *J. Exp. Med.* **170,** 1369–1385
43. Crocker, P. R. (2002) *Curr. Opin. Struct. Biol.* **12,** 609–615
44. Colonna, M., Nakajima, H., and Cella, M. (2000) *Semin. Immunol.* **12,** 121–127
45. Liu, Y., Buhring, H. J., Zen, K., Burst, S. L., Schnell, F. J., Williams, I. R., and Parkos, C. A. (2002) *J. Biol. Chem.* **277,** 10028–10036
46. Meyaard, L., Adema, G. J., Chang, C., Woollatt, E., Sutherland, G. R., Lanier, L. L., and Phillips, J. H. (1997) *Immunity* **7,** 283–290
47. Iwai, Y., Okazaki, T., Nishimura, H., Kawasaki, A., Yagita, H., and Honjo, T. (2002) *Immunol. Lett.* **83,** 215–220
48. Washington, A. V., Quigley, L., and McVicar, D. W. (2002) *Blood* **100,** 3822–3824
49. Fournier, N., Chalus, L., Durand, I., Garcia, E., Pin, J. J., Churakova, T., Patel, S., Zlot, C., Gorman, D., Zurawski, S., Abrams, J., Bates, E. E., and Garrone, P. (2000) *J. Immunol.* **165,** 1197–1209
50. Kumagai, H., Oki, T., Tamitsu, K., Feng, S. Z., Ono, M., Nakajima, H., Bao, Y. C., Kawakami, Y., Nagayoshi, K., Copeland, N. G., Gilbert, D. J., Jenkins, N. A., Kawakami, T., and Kitamura, T. (2003) *Biochem. Biophys. Res. Commun.* **307,** 719–729
51. Ishida, Y., Agata, Y., Shibahara, K., and Honjo, T. (1992) *EMBO J.* **11,** 3887–3895

52. Katz, H. R. (2002) *Curr. Opin. Immunol.* **14,** 698–704
53. Liang, S. C., Latchman, Y. E., Buhlmann, J. E., Tomczak, M. F., Horwitz, B. H., Freeman, G. J., and Sharpe, A. H. (2003) *Eur. J. Immunol.* **33,** 2706–2716
54. Batra, S. K., Metzgar, R. S., and Hollingsworth, M. A. (1991) *Cell Growth & Differ.* **2,** 385–390
55. Poggi, A., Pellegatta, F., Leone, B. E., Moretta, L., and Zocchi, M. R. (2000) *Eur. J. Immunol.* **30,** 2751–2758
56. Latour, S., Tanaka, H., Demeure, C., Mateo, V., Rubio, M., Brown, E. J., Maliszewski, C., Lindberg, F. P., Oldenborg, A., Ullrich, A., Delespesse, G., and Sarfati, M. (2001) *J. Immunol.* **167,** 2547–2554
57. Zocchi, M. R., Pellegatta, F., Pierri, I., Gobbi, M., and Poggi, A. (2001) *Eur. J. Immunol.* **31,** 3667–3675
58. Ortega Soto, E., and Pecht, I. (1988) *J. Immunol.* **141,** 4324–4332
59. Huang, Z. Y., Hunter, S., Kim, M. K., Indik, Z. K., and Schreiber, A. D. (2003) *J. Leukocyte Biol.* **73,** 823–829
60. Han, X., Sterling, H., Chen, Y., Saginario, C., Brown, E. J., Frazier, W. A., Lindberg, F. P., and Vignery, A. (2000) *J. Biol. Chem.* **275,** 37984–37992
61. Willment, J. A., Lin, H.-H., Reid, D. M., Taylor, P. R., Williams, D. L., Wong, S. Y., Gordon, S., and Brown, G. D. (2003) *J. Immunol.* **171,** 4569–4573
62. Taylor, P. R., Brown, G. D., Reid, D. M., Willment, J. A., Martinez-Pomares, L., Gordon, S., and Wong, S. Y. (2002) *J. Immunol.* **169,** 3876–3882
63. Le Drean, E., Vely, F., Olcese, L., Cambiaggi, A., Guia, S., Krystal, G., Gervois, N., Moretta, A., Jotereau, F., and Vivier, E. (1998) *Eur. J. Immunol.* **28,** 264–276
64. Henshall, T. L., Jones, K. L., Wilkinson, R., and Jackson, D. E. (2001) *J. Immunol.* **166,** 3098–3106
65. Uehara, T., Blery, M., Kang, D. W., Chen, C. C., Ho, L. H., Gartland, G. L., Liu, F. T., Vivier, E., Cooper, M. D., and Kubagawa, H. (2001) *J. Clin. Invest.* **108,** 1041–1050
66. Tooze, R. M., Doody, G. M., and Fearon, D. T. (1997) *Immunity* **7,** 59–67
67. Shimaoka, T., Kume, N., Minami, M., Hayashida, K., Sawamura, T., Kita, T., and Yonehara, S. (2001) *J. Immunol.* **166,** 5108–5114
68. Lian, R. H., Freeman, J. D., Mager, D. L., and Takei, F. (1998) *J. Immunol.* **161,** 2301–2306
69. Mason, L. H., Willette-Brown, J., Anderson, S. K., Alvord, W. G., Klabansky, R. L., Young, H. A., and Ortaldo, J. R. (2003) *J. Immunol.* **171,** 4235–4242
70. Kataoka, H., Kume, N., Miyamoto, S., Minami, M., Murase, T., Sawamura, T., Masaki, T., Hashimoto, N., and Kita, T. (2000) *J. Biol. Chem.* **275,** 6573–6579
71. Iizuka, K., Naidenko, O. V., Plougastel, B. F., Fremont, D. H., and Yokoyama, W. M. (2003) *Nat. Immunol.* **4,** 801–807
72. van der Merwe, P. A., McPherson, D. C., Brown, M. H., Barclay, A. N., Cyster, J. G., Williams, A. F., and Davis, S. J. (1993) *Eur. J. Immunol.* **23,** 1373–1377
73. Sinclair, N. R. (2000) *Crit. Rev. Immunol.* **20,** 89–102
74. Muller, A., Rice, P. J., Ensley, H. E., Coogan, P. S., Kalbfleish, J. H., Kelley, J. L., Love, E. J., Portera, C. A., Ha, T., Browder, I. W., and Williams, D. L. (1996) *J. Immunol.* **156,** 3418–3425